A Novel Design Method for Nonuniform Lattice Structures Based on Topology Optimization

Article *in* Journal of Mechanical Design · June 2018

DOI: 10.1115/1.4040546

2 authors, including:

Yafeng Han
Beijing Institute of Technology
25 PUBLICATIONS **527** CITATIONS

SEE PROFILE

A Novel Design Method for Nonuniform Lattice Structures Based on Topology Optimization

Yafeng Han
Mem. ASME
Department of Mechanical Engineering,
National University of Singapore,
9 Engineering Drive 1,
Singapore 117575
e-mail: yafenghan@u.nus.edu

Wen Feng Lu[1]
Mem. ASME
Department of Mechanical Engineering,
National University of Singapore,
9 Engineering Drive 1,
Singapore 117575
e-mail: mpelwf@nus.edu.sg

Lattice structures are broadly used in lightweight structure designs and multifunctional applications. Especially, with the unprecedented capabilities of additive manufacturing (AM) technologies and computational optimization methods, design of nonuniform lattice structures has recently attracted great research interests. To eliminate constraints of the common "ground structure approaches" (GSAs), a novel topology optimization-based method is proposed in this paper. Particularly, the structural wall thickness in the proposed design method was set as uniform for better manufacturability. As a solution to carry out the optimized material distribution for the lattice structure, geometrical size of each unit cell was set as design variable. The relative density model, which can be obtained from the solid isotropic microstructure with penalization (SIMP)-based topology optimization method, was mapped into a nonuniform lattice structure with different size cells. Finite element analysis (FEA)-based homogenization method was applied to obtain the mechanical properties of these different size gradient unit cells. With similar mechanical properties, elements with different "relative density" were translated into unit cells with different size. Consequently, the common topology optimization result can be mapped into a nonuniform lattice structure. This proposed method was computationally and experimentally validated by two different load-support design cases. Taking advantage of the changeable surface-to-volume ratio through manipulating the cell size, this method was also applied to design a heat sink with optimum heat dissipation efficiency. Most importantly, this design method provides a new perspective to design nonuniform lattice structures with enhanced functionality and manufacturability.
[DOI: 10.1115/1.4040546]

Keywords: nonuniform lattice structure, topology optimization, uniform wall-thickness, size gradient, multifunctional design, additive manufacture

1 Introduction

Lattice structures have numerous good properties, such as efficient load support, high energy absorption, and good thermal insulation [1,2]. These structures can be mainly divided into two categories, stochastic (e.g., foams) and periodic (e.g., lattice). Generally, lattice structures have higher strength-to-weight ratio comparing with stochastic structures [3]. Deshpande et al. [4] demonstrated that open cell lattice structures with $\rho = 0.1$ has shown at least a 300% increase in structural performance over typical foam structures with same relative density. Another advantage of lattice structure is for each unit cell, and even each strut in the structure can be set as the design variable and be optimized to achieve the desired customized requirements. All those advantages provide lattice structures great potential in a wide range of applications, such as automobile, aerospace, medical devices, and bio-implants [5].

Conventionally, lattice structure design is mainly focused on adjusting geometries of the single unit cell, and then on building a structure with repeated uniform cells. The primary reason is that design freedom is strictly constrained by the manufacturability of traditional manufacturing processes [6], and only simple and uniform lattice structures can be fabricated without much difficulty. The most typical example of such processes is honeycomb structure manufacturing. Not only having longer time and higher cost for fabrication, traditional processes also limit the possibility of fabricating nonuniform lattice structures. With rapidly developing additive manufacturing (AM) technologies, the manufacturing barriers have been overcome to make a huge difference on developing better performance lattice structures [7,8]. The unique manufacturing mechanism of joining materials layer by layer, or point by point, gives AM the capability to fabricate complex structures without additional cost [9].

With these unique capabilities of AM, many studies have focused on the design of nonuniform lattice structures. "Ground structure approaches" (GSAs) [10] are the most common methods. With predefined "ground structure" in the design domain, one or several parameters of each unit cell or strut can be numerically optimized to fulfil the design objective. Traditionally, size optimization [11] method was applied to design nonuniform lattice structures. In Rosen's research [3], the author proposed an evolutionally method to optimize the diameter of each strut in a lattice structure. The obtained structure had better mechanical properties and lower material cost, compared with the uniform ones. For better structural performance, Gilbert and Tyas [12] discretized the design domain into very fine sections and applied fully connected ground structure to conduct the size optimization. Particularly, all thin struts were eliminated to achieve layout optimization. The resulting structure can almost achieve the theoretical optimum, as long as the number of connection nodes in the design domain is large enough. Several similar methods [13–15] were also proposed. All these methods have tried to minimize the constraint of ground structure through increasing the number of connection nodes and applying fully connected ground structure. However, this will lead to extra presetting steps during the

[1]Corresponding author.

Contributed by the Design Automation Committee of ASME for publication in the Journal of Mechanical Design. Manuscript received February 1, 2018; final manuscript received June 6, 2018; published online July 9, 2018. Assoc. Editor: Nam H. Kim.

problem definition process. Besides, construction of ground structure will become extremely complex when the given design domain is an irregular shape.

The fast developing topology optimization techniques [11] provided new opportunities to conduct high-efficiency GSAs. Considering the hypothetical "relative density" model is difficult to be manufactured directly [16,17], translating the "relative density" information into a manufacturable lattice structure becomes a better choice [7]. Zhang and Sun [18] introduced a two-level design method that combines macroscale layout optimization and microstructure design. However, this method can only be applied to extremely simple loading case of two-dimensional (2D) problems. In order to extend the design flexibility and develop a "systematic approach," Alzahrani et al. [19] conducted a relative density mapping method to determine the appropriate thickness of each lattice strut. In this method, continuous topology optimization is applied to obtain the best material distribution in design domain, and the material density model is remapped to a predefined lattice "ground structure." Similarly, Zhang et al. [20] developed a novel remapping method to obtain a variable-density hexagonal lattice structure, which can be easily fabricated by stereolithography.

High computational efficiency is the main advantage of topology optimization-based GSAs. However, the drawback is obvious that predefined "ground structure" highly restricts the design freedom. Besides, almost all these methods did not consider the manufacturability of the obtained lattice structure. With nonuniform wall thickness, it is impractical for these optimized lattice structures to be mass-fabricated by traditional manufacturing processes, such as injection modeling [21]. Even with much higher manufacturability of AM processes, they also have minimum wall-thickness constraints [22]. Especially, for laser additive manufactured metallic components, variation of wall thickness may cause uneven heat dissipation, and lead to undesired thermal deformation [23]. Another deficiency of aforementioned topology optimization-based methods is the focus on the equivalent transformation of material "relative density," but not material property. As a result, the obtained lattice structure may have a similar material distribution as the topology optimization result. However, the mechanical property of the obtained structure, which should be the priority, cannot be ensured.

To eliminate design constraints of the predefined "ground structure" and enhance the functionality and manufacturability, a novel nonuniform lattice structure design method is proposed in this paper. Specifically, the proposed method aims at generating nonuniform lattice structures with uniform wall thickness for better manufacturability. For load-support structures, it is obvious that small unit cells have high Young's modulus and large unit cells have low Young's modulus. Consequently, the distribution of different size unit cells can be optimized to achieve the design objective. By locating unit cells at areas where they have similar elements' Young's modulus, the topology optimized "relative density model" can be transferred into a distribution of different size unit cells. Utilizing the material Young's modulus as the transfer media, not "relative density," generates the mechanical properties of the generated lattice structure closer to the topology optimization result. Besides, to ensure the design domain is fully covered by unit cells, the cell size needs to be discretized into several gradients, and all size gradients should be integral multiples of the smallest one. As a result, the proposed size gradient method (SGM) can obtain a nonuniform lattice structure, which has an optimized distribution of unit cells with different size and constant wall thickness. Because wall thickness is maintained as uniform, the generated lattice structure has much better manufacturability, and can be easily fabricated by both traditional injection molding and AM processes. Two validation examples, cantilever beam and compliance force inverter, were designed and analyzed both numerically and experimentally. Apart from load-support designs, a three-dimensional (3D) lattice heat sink with optimized heat dissipation ability was also developed.

The proposed SGM was illustrated in Sec. 2. To illustrate the proposed method thoroughly, technical details were discussed in Secs. 3–5, along with validation examples in Sec. 6.

2 Proposed Size Gradient Method

The main objective of the proposed SGM is to generate a nonuniform lattice structure with optimized distribution of different size unit cells. Systematically, this optimization problem can be represented as

$$\text{optimize}: StuP = \sum_{c=1}^{n} CelP_c = \sum_{c=1}^{n} Homo\{CelG_c(EleP_{TPO}^{avg})\} \tag{1}$$

where $StuP$ denotes the structural property that needs to be optimized. n is the total number of unit cells in the lattice structure. Property of each cell $(\mathrm{Ce}lP)$ can be obtained from homogenization analysis of each size gradient $(\mathrm{Ce}lG)$. With similar average element property $(EleP_{TPO}^{avg})$ from topology optimization, corresponding unit cell $(CelG_c)$ can be fitted into the design domain. Considering the optimization of material distribution is mainly achieved through traditional topology optimization process, efficiency, and robustness of the proposed SGM can be maintained. By applying different size unit cells to reinterpreting the relative density model, manufacturability of the generated structure can be ensured. The proposed method composes of five steps, as shown in Fig. 1.

(i) *Initial design specification*. Similar to all structural design problems, first step of SGM is to provide the specification of initial design conditions. As the proposed method is a "generative" method based on topology optimization, there is no need to predefine any "ground structure" as other traditional lattice design methods. Only simple analysis of load and boundary conditions are necessary for SGM.

(ii) *Topology optimization:* To obtain the objective of distributing materials to where they are needed, solid isotropic microstructure with penalization (SIMP) [11] method was adopted in SGM to conduct topology optimization. The only difference is that Young's modulus, not "relative density," of each element in the design domain is considered during the optimization.

(iii) *Size gradient definition and unit cell homogenization:* In this step, topology, material, wall thickness, and size gradients of the unit cells are predefined. Face centered square (FCS) unit cell is chosen to construct the structure, and connectivity of the final structural is considered. Materials and wall thickness of structures are determined according to capabilities of the selected AM process. Size gradients are determined based on the geometrical size and complexity of the design domain. Homogenization analysis [24], which utilized a homogenized continuous solid to approximately represent a lattice unit cell, is applied to obtain mechanical properties of unit cells with different sizes.

(iv) *Lattice structure generation:* Based on the topology optimization result from step (ii) and unit cells' Finite element analysis (FEA) results from step (iii), the nonuniform lattice structure can be generated by positioning different size unit cells at corresponding areas with similar Young's modulus. Particularly, cell size is set as gradient to achieve complete coverage of the design domain. As a result, Young's modulus of different size gradient unit cells is also not continuously changed. Considering that the "relative density" in topology optimization result is varied continuously, approximation is needed to assign each gradient cell to cover a value range around its particular Young's modulus.

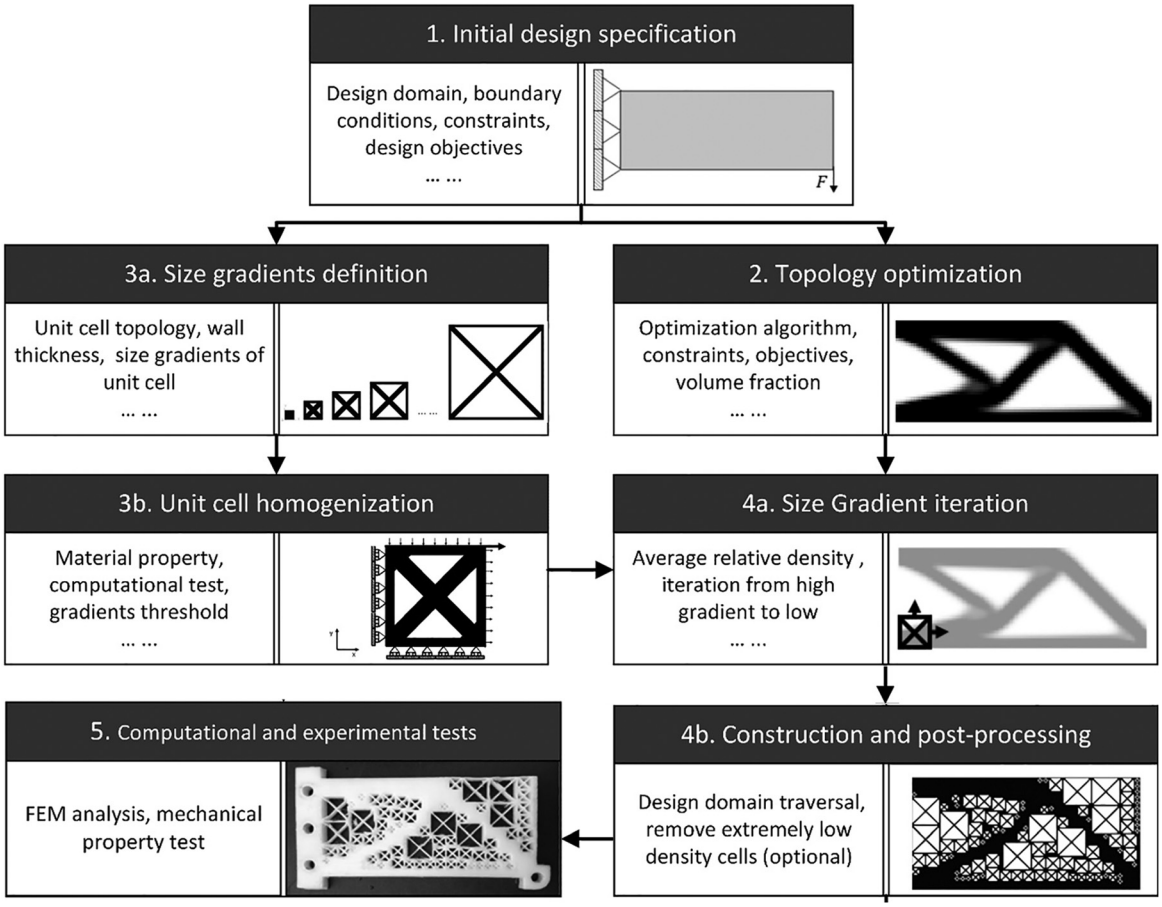

Fig. 1 Overview of SGM

3 Topology Optimization

To find the best material distribution for specific design requirements, numerous structural optimization methods have been developed. Generally, these methods perform three different types of objectives: size, shape, and topology optimization [11]. Figure 2 shows Bendsøe and Sigmund's [11] interpretation of these three different kinds of methods. Size optimization is the most common method utilized in traditional lattice structure design area [3]. Always, a "ground structure" is predefined in the design domain, and the diameter or the thickness of each strut is optimized to achieve the design objective [25]. With higher flexibility, shape optimization only needs to preset the objective topology of the structure. By controlling vertices of parametric curves or surface of these "holes," optimized material distribution of the structure can be achieved. Huge numbers of design variables, which lead to dramatically computational cost, are the main obstacle for these two methods to achieve pervasive application. In addition, predefined "ground structure" or topology also limits the flexibility of optimization, especially when considering the unprecedented manufacturability brought by AM.

Different from size and shape optimization, topology optimization deals with the topology of the structure directly to achieve the objective of "putting material where it is needed" [3]. This optimization method was first proposed in the 1980s and has a noticeable development in last decades. Different techniques and algorithms

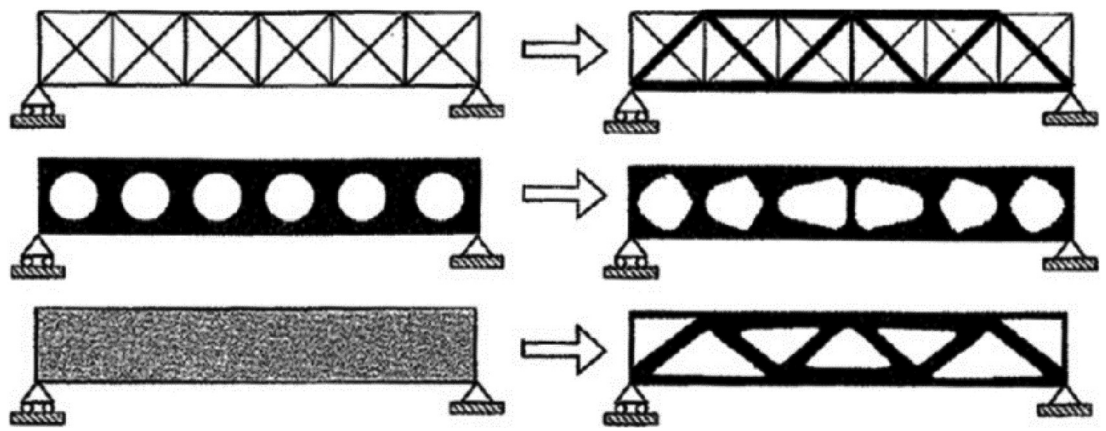

Fig. 2 Size (top), shape (middle), and topology (bottom) optimization [11]

have been proposed, such as SIMP [11], genetic algorithms [26], and level set [27]. Particularly, SIMP is one of the most well developed homogenization-based methods [28]. To conduct this method, linear elastic FEA is introduced to analyze the structure, and Young's modulus of each element E_e in the design domain is homogenized as isotropic. As a result, energy bilinear form of the structure can be represented as

$$\int_S \mathbf{f}^T \mathbf{u} dS = \frac{1}{2} \sum_{e=1}^{N} \mathbf{u}_e^T \mathbf{k}(E_e) \mathbf{u}_e \tag{2}$$

where S is the structural boundary, $\mathbf{f}$ is the external loading vector, $\mathbf{u}$ and $\mathbf{u}_e$ are global and element displacement vectors accordingly. With the assumption of linear elastic, the element stiffness matrix $\mathbf{k}(E_e)$ is linearly related with element Young's modulus E_e. Usually, a hypostatical element "relative density" ρ_e is applied for a better represent of E_e

$$E_e = (\rho_e)^p E_0 \tag{3}$$

In Eq. (3), p is the penalty factor, which is typically set as $p = 3$ for higher convergence rate and better material layout. The available range of ρ_e is set from 0.01 to 1 in this paper. E_0 is the base material Young's modulus of the designed lattice structure.

Initially, SIMP method is applied to solve minimum compliance design. As demonstrated in Ref. [29], the mathematic representation of minimum compliance problem is

$$\begin{aligned} \min_{\rho} \quad & : c(\rho) = \sum_{e=1}^{N} (\rho_e)^p \mathbf{u}_e^T \mathbf{k}(E_e) \mathbf{u}_e \\ \text{subject to} \quad & : V(\rho)/V_0 = f_v \\ & 0.01 \le \rho_e \le 1 \end{aligned} \tag{4}$$

where c is the compliance of the structure, f_v is the prescribed volume fraction. With different f_v, the number of different size unit cells in the lattice structure will be changed. However, the material distribution from topology optimization can still be represented. In Sec. 6.1, a minimum compliance design of a 2D beam structure is used to test the proposed SGM method. Besides, SIMP method can also be modified to solve different design problems. Accordingly, robust, multimaterial SIMP approach [30] is conducted to design a compliant force invertor as shown in Sec. 6.2, and 3D heat conduction SIMP method [31] is applied to design a CPU heat sink in Sec. 6.3.

4 Size Gradient Definition and Unit Cell Homogenization

In this paper, 2D FCS unit cell was selected to construct the lattice structure. To make sure there are no remaining gaps in the generated lattice structure, all unit cell sizes should be discretized into gradients and set as integral multiples of the smallest one. As shown in Fig. 3, the size gradients were predefined as from (1×1) to (10×10) unit length. Specifically, wall thickness was assigned as 0.5 unit length for the consideration of the manufacturability. Consequently, the first grade (1×1) cell is actually a solid square.

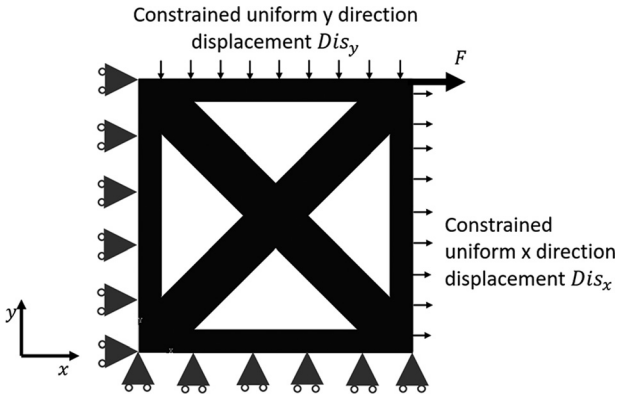

Fig. 4 Load and boundary condition of cell homogenization analysis

Considering the mechanical properties of FCS are nonlinear and anisotropic, homogenization method [24] was applied to analyze these unit cells. There are mainly two ways to perform homogenization: one is to use mathematical formulation [28,32] to predict structure properties; the other way is to conduct numerical or experimental sample testing [33]. For the proposed SGM, the latter method was utilized, and structural Young's modulus and Poisson's ratio of each gradient were obtained through FEA. Same as Sun and Vaidya's [33], loading and boundary conditions of the homogenization analysis were set as stated in Fig. 4.

With an assumed unit at which Young's modulus $E_0 = 1$ and Poisson's ratio $\nu_0 = 0.3$, mechanical properties of each size gradient can be analyzed. Linear FEA was run on ABAQUS, and obtained cell Young's modulus E_c and Poisson's ratio ν_c were calculated through the following equations:

$$E_c = F/Dis_x \tag{5}$$

$$\nu_c = -Dis_y/Dis_x \tag{6}$$

Finite element analysis results of all gradient cells are listed in Table 1. As can be observed, the Poisson's ratio of each gradient does not have much difference, only Young's modulus of was considered during the translation from topology optimization result to the nonuniform lattice structure. As shown in Fig. 5, the test results can be perfectly fitted into an exponential function

$$E_c = 1.0757 \times G_c^{-1.15} \tag{7}$$

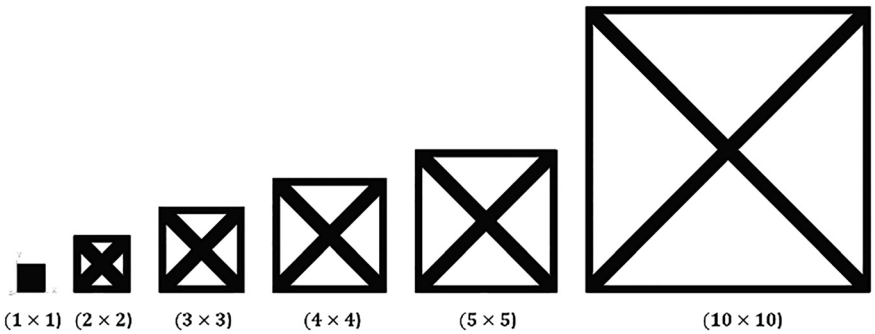

Fig. 3 Predefined FCS cells with different size gradients

Table 1 FEA-based homogenization results of each size gradient

Gradient (G_c)	1	2	3	4	5	10
Cell size (unit length)	1×1	2×2	3×3	4×4	5×5	10×10
Young's modulus (E_c)	1.00	0.55	0.30	0.21	0.17	0.07
Poisson's ratio (ν_c)	0.33	0.33	0.34	0.34	0.35	0.35
Thresholds for E_e	$(0.68, 1]$	$(0.38, 0.68]$	$(0.26, 0.38]$	$(0.19, 0.26]$	$(0.11, 0.19]$	$[0, 0.11]$
Thresholds for ρ_e	$(0.88, 1]$	$(0.72, 0.88]$	$(0.64, 0.72]$	$(0.57, 0.64]$	$(0.48, 0.59]$	$[0.01, 0.48]$

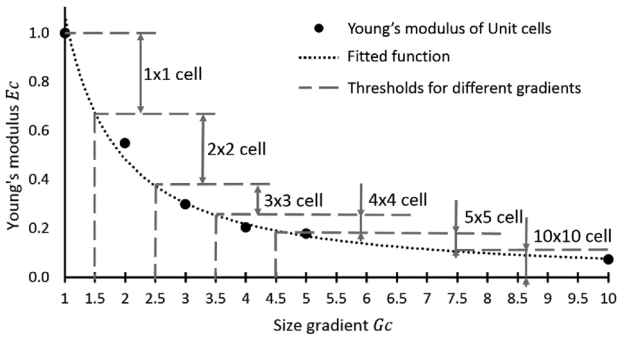

Fig. 5 Test results and fitted curve of the correlation between size gradient and unit cell Young's modulus

where G_c denotes the size gradient. Obviously, with cell size growing, the value difference of Young's modulus between each gradient becomes smaller. That is the reason why gradients between $G_c = 5$ to $G_c = 10$ were neglected (as shown in Fig. 3).

With the obtained "size gradient-Young's modulus" relation (Eq. (6)), unit cells with different size gradients can be utilized to map a topology optimized material distribution into a nonuniform lattice structures. However, the variation of unit cell Young's modulus E_c was discretized into gradients, while element Young's modulus E_e was continuously changed. As a solution, each gradient should cover a proper range of average element Young's modulus E_e. In the proposed method, Young's modulus of medium values between each gradient were calculated and set as thresholds, as shown in Fig. 5. The exact ranges of each interval are summarized in Table 1. With penalty factor set as p = 3, the corresponding element relative density ρ_e is also listed.

5 Nonuniform Lattice Structure Generation

With the equivalent transformation between element relative density ρ_e and cell size gradient G_c, the optimized lattice structure can be constructed. The general process is illustrated in Fig. 6. To place different gradient cells at their best locations, size gradient iteration and design domain traversal are the two main procedures. The iteration is done from the largest size gradient ($G_c = 10$) to the smallest one ($G_c = 1$), and the traversal is done from left to right (direction of $+x$) and down to top (direction of $+y$). During iteration of each gradient, according unit cell will traverse the whole design domain, and substitute the elements when their average density ρ_e^{avg} lies in corresponding interval from Table 1. Figure 6(*b*) shows how a 3×3 cell is generated in the design domain. After the iterations of $G_c = 10, 5,$ and 4, traversal of the 3×3 cell was processed over the design domain. With the area enclosed by dotted line as shown in Fig. 6(*b*), the average density $\rho_e^{\text{avg}} = 0.682$, which is in the range of $(0.66, 0.76]$. Consequently, a $G_c = 3$ unit cell was generated in this area.

With iterations done from larger gradients to smaller ones, the remaining gaps will all be filled with different size unit cells and the optimized nonuniform lattice structure can be constructed. Traversal order and direction may have slight influence on the result, but the objective of optimization can always be achieved. Such as the 2D beam design in Sec. 6.1, the difference of structural compliance caused by different traversal directions ($+x$,$+y$ and $-x$, $-y$) is 1.4%, and the difference caused by different traversal orders (small to large & large to small) is 2.8%. Besides, filling all the remaining gaps with very small cells may cause small incensement on volume fraction of the generated lattice structure. Nevertheless, our focus is on achieving objective mechanical performance, volume fraction is just the secondary consideration.

6 Demonstration Examples

6.1 Cantilever Beam Design. Simple beam is a benchmark test for lattice structure design and many research [19,20] in this area have utilized this test for validation. In this paper, a simple cantilever beam was analyzed and optimized. As shown in Fig. 7, the beam has length $l = 80$ mm, height $h = 40$ mm, and width $b = 3$ mm. At lower right corner, a load $F = 200$ N is applied. The design objective is to minimize the compliance of the beam structure.

As introduced in Sec. 4, SIMP method was applied to optimize the beam structure. The volume fraction was set as $f_v = 0.5$, and penalty factor as $p = 3$. The "relative density" model of optimization result is shown in Fig. 8(*a*). With the topology optimization

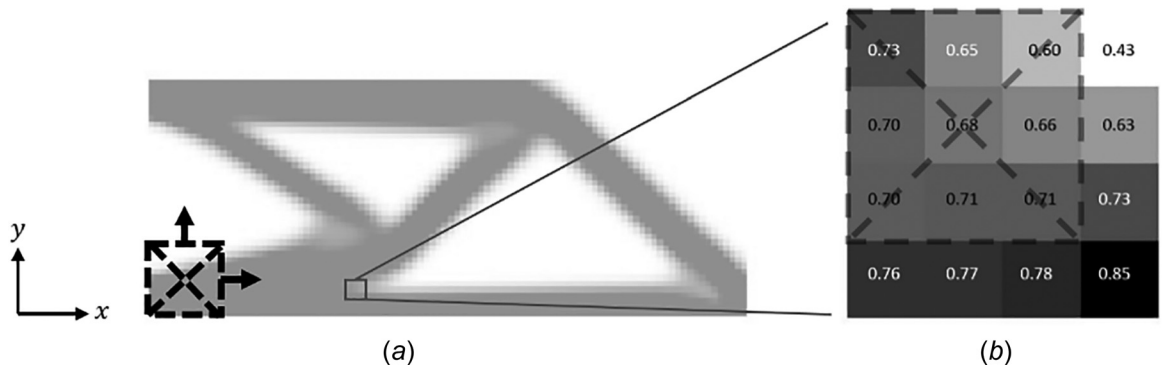

Fig. 6 Lattice structure generation process: (*a*) shows the traversal direction ($+x$, $+y$) of each gradient and (*b*) shows the detailed generation process of a 3×3 cell

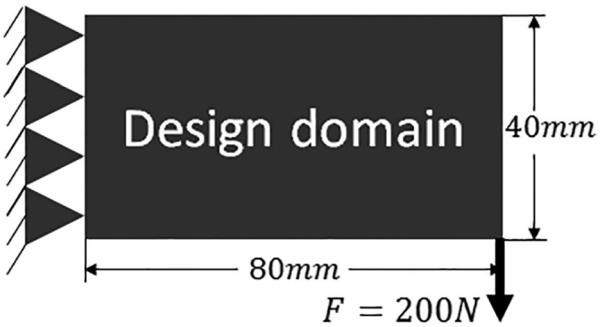

Fig. 7 Initial conditions of cantilever beam design

result, the optimized lattice structure can be generated based on the "cell size gradient-element density relation" as shown in Table 1. After size gradient iteration and design domain traversal, the final optimized lattice structure of the aforementioned cantilever beam is shown in Fig. 8(*b*). It can be observed that small error occurred near the right edge area, which is inevitable in SGM. Consequently, the volume fraction of the optimized lattice structure is 0.51, which is higher than initial topology optimization result.

VeroWhitePlus, which can be easily additive manufactured, was applied to fabricate the lattice. With a Young's modulus of $E_0 = 2500$ MPa and Poisson's ratio of $\nu_0 = 0.3$, FEA was done in ABAQUS to validate whether the optimized lattice structure has a smaller compliance than a uniform structure with same material cost. 4-node bilinear plane stress quadrilateral element was applied to mesh all these three parts. The detailed test data are summarized in Table 2. The result shows that SGM result has much smaller compliance compared with uniform lattice structure, and the structural performance is almost as good as the topology optimization result.

Further confirmation for the SGM method was carried out via experimental test. Both optimized and uniform lattice beams were printed using a Stratasys® Objet Connex 350 machine as shown in Fig. 9. The only difference is the additional features added to each beam in order to provide a feature for fixture and load to be applied. The tensile test is done on an Instron® MODEL 5500 material testing system. A crosshead motion rate of 1 mm/min was applied, and the maximum load was set as 200 N. With customized fixture and cylindrical pin, the test can be carried out. Figure 10 demonstrates the test results, in which the final tip displacements were marked. Obviously, the SGM optimized lattices have much better performance than the uniform one. However, because of the inherent material porosity of PolyJet process and edge damages caused by support removing process, both experiment tests have larger compliance compared with corresponding FEA results.

6.2 Compliant Mechanism Design. Apart from minimum compliance design, the proposed SGM can also be applied to design compliant mechanisms. Usually, topology optimized compliant mechanisms need relatively low volume fraction to achieve

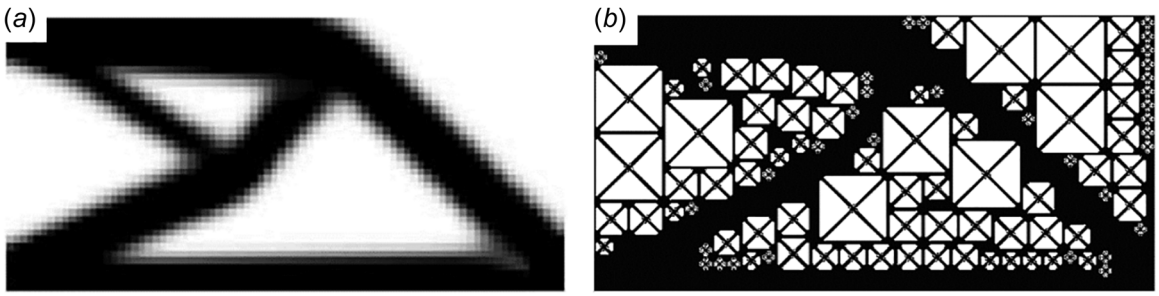

Fig. 8 (*a*) is the conventional topology optimization result and (*b*) is the SGM generated nonuniform lattice structure

Table 2 Comparison of FEA test results for three different beam construction methods

Method	Volume fraction	Tip displacement (mm)	Structural compliance (mm/N)
Topology optimization	0.5	2.07	0.01075
Uniform	0.51	3.51	0.01755
SGM	0.51	2.21	0.01105

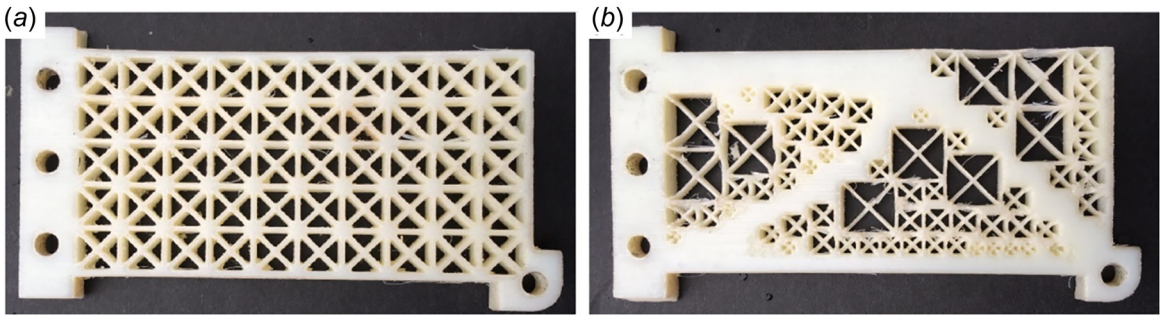

Fig. 9 Testing samples that fabricated by Objet Connex 350: (*a*) is the comparison structure with uniform lattice size and same material cost and (*b*) is the optimized lattice structure

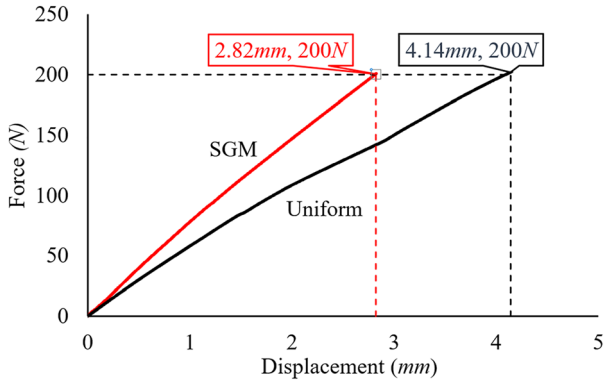

Fig. 10 Tensile test results of both uniform and optimized non-uniform lattice structure

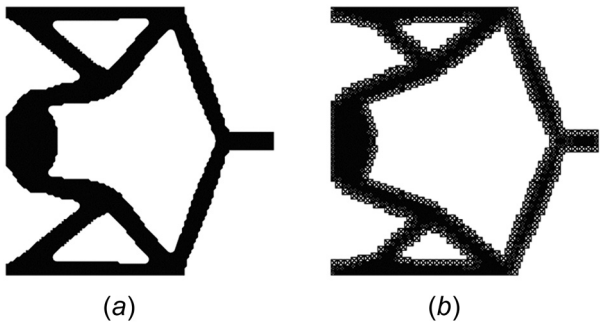

Fig. 12 (*a*) Topology optimization result fabricated with single material and (*b*) single material lattice inverter generated by SGM

Table 3 FEA test results of three different force inverters

Method	Tip displacement (mm)
Two-material solid	2.73414
Single-material solid	1.76917
SGM lattice (single material)	2.55573

better performance. To obtain lattice structures with such a high percentage of "void" areas, SGM can be modified to achieve free form boundaries, by eliminating high gradient cells and only generating cells in relatively high-density area.

In this paper, a complaint force invertor was selected to validate the proposed SGM. This particular compliant mechanism was initially introduced by Sigmund [34], and has become one of the benchmark problems for topology optimization. Referring to Gaynor et al. [35] research about the same problem, robust, multi-material SIMP approach [30] was chosen to optimize the structure. Dimensions of the design domain and boundary conditions are presented in Fig. 11(*a*). With a constant input force of $F_{\text{in}} = 100\text{N}$ and spring constant $k_{\text{out}} = 1\text{N/mm}$, the optimization objective is to maximum the output displacement U_{out}. The structure thickness was 3mm, and the volume fraction was set as $f_v = 0.3$. Particularly, two kinds of materials, hard material (Vero-WhitePlus) with Young's modulus of $E_0^H = 2500$ MPa and soft material with $E_0^S = 1250$ MPa, were selected to construct the structure. Besides, length scale variation was set as 9mm to eliminate "one-node hinge" phenomena. Figure 11(*b*) displays the solution of this robust, multi-material topology optimization.

The design result shows large percentage of "void" areas and thin features, as most compliant mechanisms do. To construct a reasonable lattice structure based on this material distribution, larger gradient cells were unnecessary, and only gradients of $G_c = 1, 2$ and 3 were considered. Based on Table 1, the relative density model was successfully mapped into a lattice structure as shown in Fig. 12(*b*). This lattice structure shared similar outer boundary with the single-material fabricated topology optimization result (Fig. 12(*a*)). Same as the cantilever beam example, computational test was first conducted to compare performance of the two-material solid structure, single-material solid structure and SGM generated lattice structure. Same element type was also applied. Table 3 shows the tip displacement of these three structures under the same F_{in}. The FEA result showed that SGM lattice structure has much better performance compared with single material topology optimized structure, even though both structures were comprised of single material.

With the same test platform and AM process as aforementioned cantilever beam test, performances of both SGM lattice force invertor and single material topology optimized force invertor were tested. The results are shown in Fig. 13, in which (a) and (c) were the initial states of two cases, (b) and (d) were obtained tip displacement of both cases under the same load. Two clamp plates were added to eliminate out-of-plane bending during the test. Because some thin walls were broken during the support removal process, both obtained displacements were slightly larger than corresponding FEA results, which was within the expectation.

6.3 Heat Sink Design. The most significant advantage of SGM in solving heat dissipation problem is the high surface-to-volume ratio at small cell areas of the generated structure. This

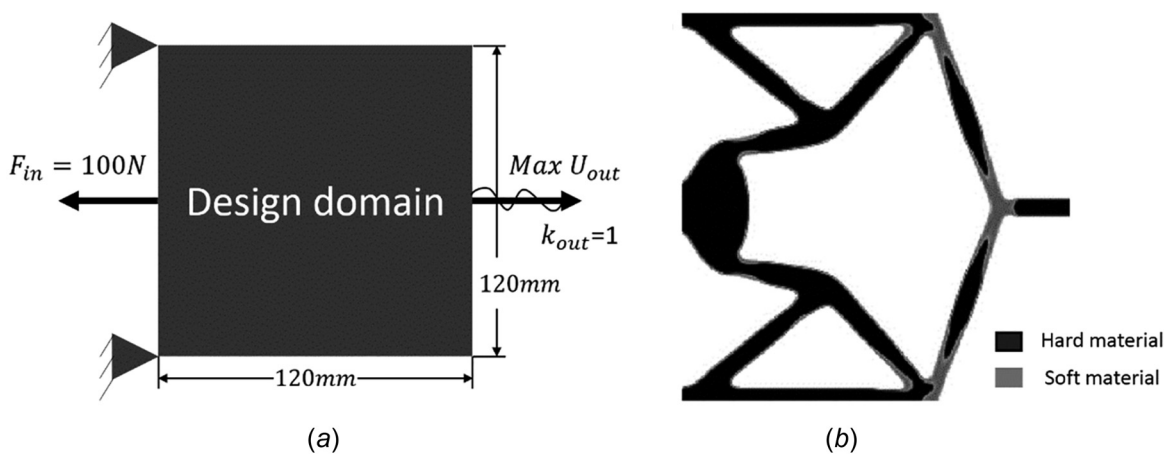

Fig. 11 (*a*) Initial conditions of compliant force inverter design and (*b*) topology optimization result with two different materials

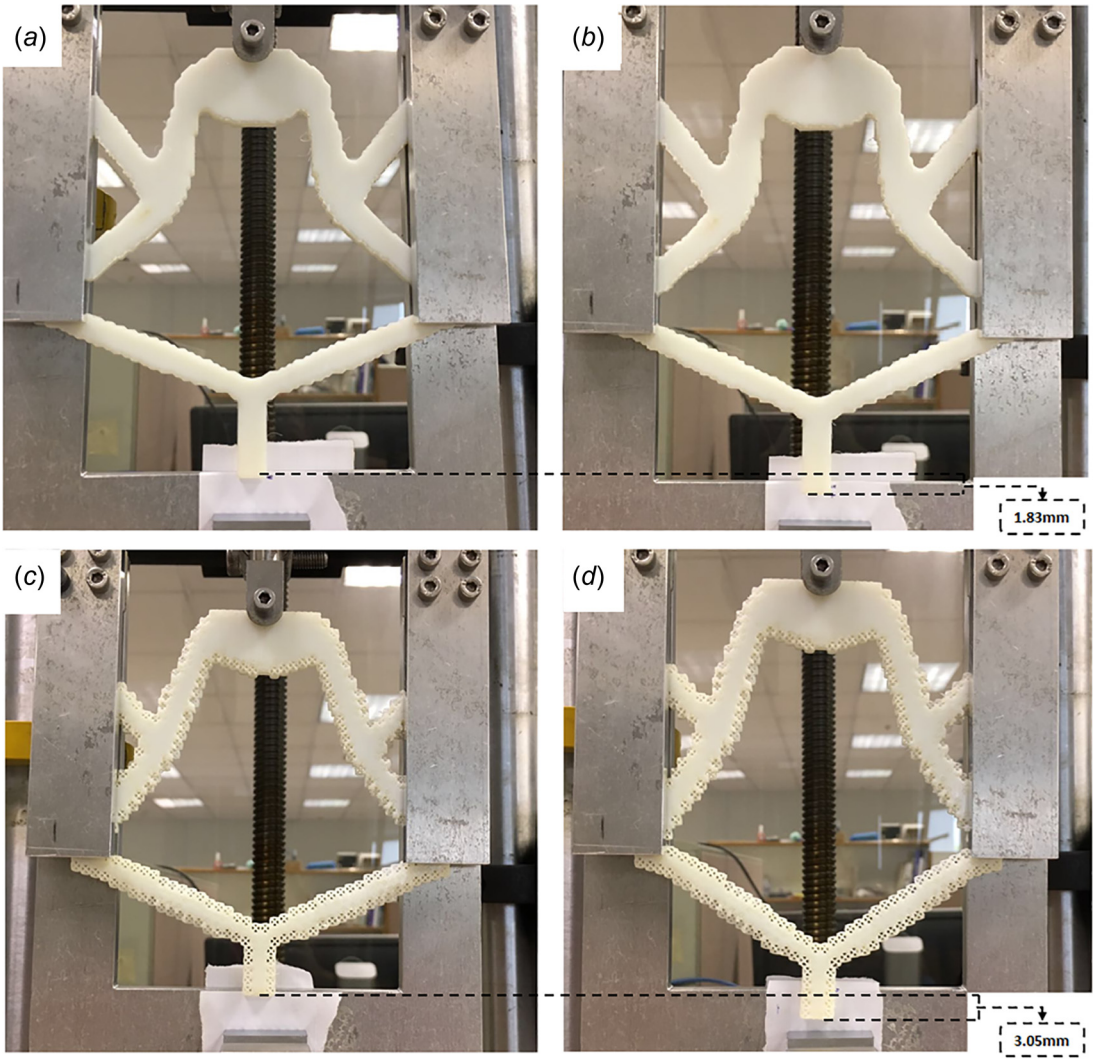

Fig. 13 Tensile tests of single material optimized solid structure and SGM generated nonuniform lattice structure

means that there will be more sink–coolant interface area at the high "relative density" region. Consequently, this will bring a higher heat dissipation efficiency to the optimized lattice structure. In this paper, the proposed SGM was introduced to construct a lattice CPU heat sink [31,36]. Initial geometries and boundary conditions are given in Fig. 14. It consists of a design domain (the upper part) of dimension $100 \times 100 \times 50$ mm^3, and an assembly area (the bottom) with the dimension of $100 \times 100 \times 5$ mm^3. A uniform surface heat flux of magnitude 0.2 W/mm^2 was applied at the middle of bottom surface with an area of 40×40 mm^2. A forced convection existed over the design domain boundaries. The optimization problem is to minimize the thermal compliance, subjected to a volume constraint of 20% of the initial volume. Other parameters are set as follows: material conductivity equals to 0.237 W/mm · K, the prescribed temperature is 20 °C, and convection coefficient between sink surface and coolant is 10^{-5} W/mm^2 · K.

The SIMP method-based topology optimization can be easily introduced to solve this minimum thermal compliance design, and the result is demonstrated in Fig. 15(*a*). 3D body-centered cubic unit cells with different size were applied to build the nonuniform lattice structure. Three different size gradients, $(5 \times 5 \times 5)$, $(10 \times 10 \times 10)$, and $(15 \times 15 \times 15)$, were applied to construct the structure. The geometry of the optimized lattice heat sink is shown in Fig. 15(*b*).

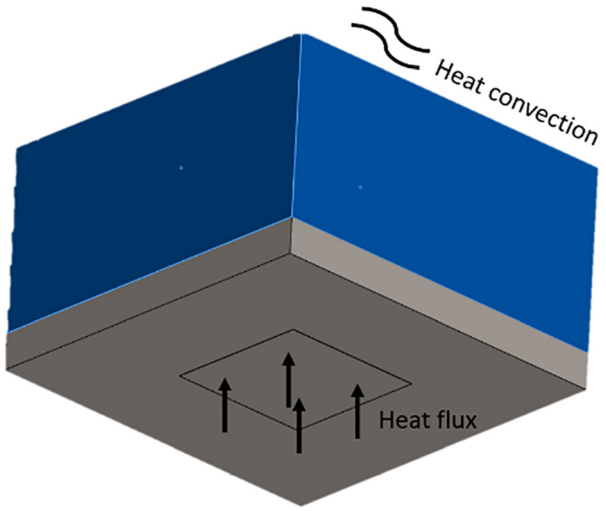

Fig. 14 Topology optimization of a passive heat sink: design domain (upper area), nondesign domain (lower area), and boundary conditions

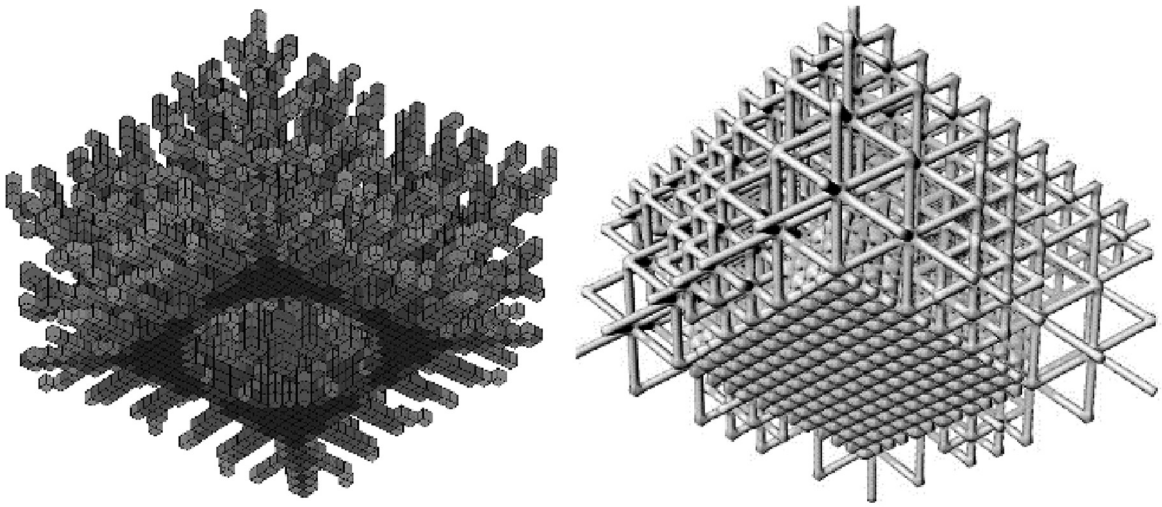

(*a*) (*b*)

Fig. 15 Optimized geometry of the design domain. (*a*) is the relative density model of the topology optimization result and (*b*) is the generated nonuniform lattice structure.

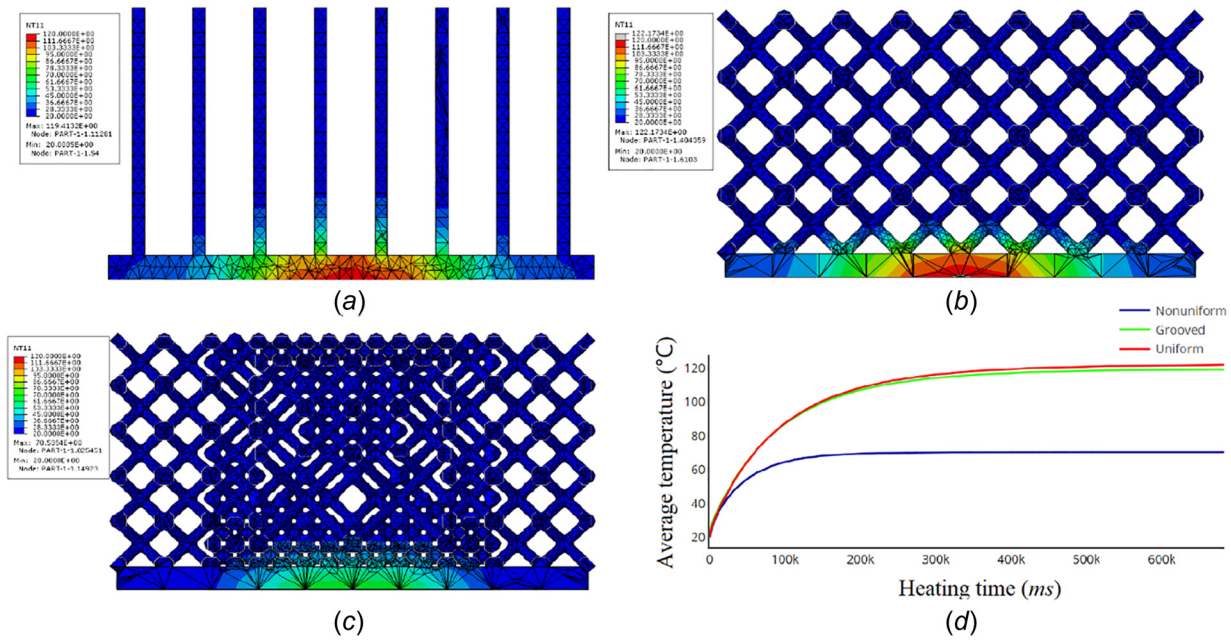

(*a*) (*b*) (*c*) (*d*)

Fig. 16 FEA results of three different heat sink designs. (*a*) is the temperature distribution of the traditional grooved structure, (*b*) is the temperature distribution of the uniform lattice structure, (*c*) is the temperature distribution of the optimized nonuniform lattice structure, and (*d*) shows the average temperature changing processes at the heat flux region of these three structures.

To test the heat dissipation performance, three different heat sink designs, traditional grooved structure, uniform lattice structure, and optimized nonuniform lattice structure, were all analyzed in ABAQUS. 4-node linear heat transfer tetrahedron element was applied to mesh all three designs. These three structures had the same volume fraction, and the FEA results are shown in Fig. 16. Besides, Fig. 16(*d*) shows the changing process of the average temperature at heat flux region of these three different designs. Obviously, the optimized nonuniform lattice structure has the highest heat dissipation efficiency. For comparison, the detailed geometry parameters and average temperatures at heat flux region are summarized in Table 4. Compared with the uniform lattice structure, the optimized structure has much higher heat dissipation efficiency, even though both structures have same volume and similar interface area with coolant.

7 Discussion and Conclusions

In this paper, a size gradient method for nonuniform lattice structure design was proposed. The proposed SGM took the advantage of high efficiency and robustness form topology

Table 4 Geometry parameters and average temperatures at heat flux region of all three heat sink designs

Model of sink	Grooved	Uniform	Nonuniform
Material volume (mm^3)	6500	6500	6500
Convection surface (mm^2)	14,014	23,067	23,440
Temp. at flux region (°C)	119.4	122.2	70.5

optimization, and got rid of the high time and computational cost of traditional size or shape optimization-based GSAs. Most importantly, SGM used uniform wall-thickness unit cells to maintain the manufacturability of the generated structure, which is totally different from common topology optimization-based GSAs. By manipulating the geometrical size, distribution of unit cells with variable structural properties was optimized for different design objectives. Particularly, the value of each unit cell's property was calculated and analyzed through FEA-based homogenization method. With the basic thought of matching different size unit cells at corresponding areas in the design domain, a nonuniform lattice structure with similar mechanical properties as the topology optimization result could be constructed. With the constraint of uniform wall thickness, the generated designs can not only be additive manufactured but also be easily fabricated by conventional manufacturing, such as injection molding. To validate the reliability and effectiveness of the proposed SGM, three different design cases, cantilever beam, force inverter, and heat sink, were introduced. Compared with original topology optimization results, properties of all designs were not as good. This loss of structural properties is inevitable, considering the gain of much better manufacturability. Commonly, the relative density model from topology optimization is very difficult to be manufactured without extra postprocessing. As a more reasonable comparison, the generated nonuniform lattice structures all have much better performance than their contrasts with uniform cell size.

This innovative lattice structural design method has its own limitations. First, the volume fraction of the obtained lattice structure cannot be exactly controlled because the translation was focused on mechanical properties, not material density. Besides, the variation of cell size was discretized into gradients, so approximation was applied to divide element density into corresponding intervals. To make this method more effective and powerful, there are some aspects need to be improved for the extensive application of SGM. Further research can be generalized but not limited to the following aspects: (1) Modifying the proposed method to solve multidisciplinary problems. Especially, with the easily control of structural surface-to-volume ratio, SGM may also have great potential in biomaterial researches. (2) Developing a unit cell library, which contains properties and capabilities of different cell structures. For example, unit cells with optimized stiffness or buckling properties can be chosen to eliminate stress and buckling constraints. Conductivity of each cell structure should be emphasized in SGM to ensure that the generated structure is continued. Besides, manufacturability of different types of cells needs to be evaluated.

References

[1] Gibson, L. J., and Ashby, M. F., 1999, *Cellular Solids: Structure and Properties*, Cambridge university press, Cambridge, UK.

[2] Wadley, H. N. G., 2002, "Cellular Metals Manufacturing," Adv. Eng. Mater, **4**(10), pp. 726–733.

[3] Rosen, D. W., 2007, "Computer-Aided Design for Additive Manufacturing of Cellular Structures," Comput. Aided. Des. Appl., **4**(5), pp. 585–594.

[4] Deshpande, V. S., Fleck, N. A., and Ashby, M. F., 2001, "Effective Properties of the Octet-Truss Lattice Material," J. Mech. Phys. Solids, **49**(8), pp. 1747–1769.

[5] Tang, Y., and Zhao, Y. F., 2015, "Lattice-Skin Structures Design With Orientation Optimization," Solid Freeform Fabrication Symposium, Aug. 10–12, Austin, TX, pp. 1378–1393.

[6] Beach, L., Figueroa, D., Engineer, D., Corporation, F. F., and Beach, L., 2016, "Design and Analysis of Lattice Structures for Additive Manufacturing," ASME J. Manuf. Sci. Eng., **138**(12), p. 121014.

[7] Dong, G., Tang, Y., and Zhao, Y. F., 2017, "A Survey of Modeling of Lattice Structures Fabricated by Additive Manufacturing," ASME J. Mech. Des., **139**(10), p. 100906.

[8] Han, Y., and Lu, W., 2017, "Evolutionary Design of Nonuniform Cellular Structures With Optimized Poisson's Ratio Distribution," Mater. Des., **141**, pp. 384–394.

[9] Gibson, I., Rosen, D., and Stucker, B., 2015, *Additive Manufacturing Technologies: 3D Printing, Rapid Prototyping, and Direct Digital Manufacturing*, 2nd ed., Springer, New York.

[10] Bendsoe, M. P., Ben-Tal, A., and Zowe, J., 1994, "Optimization Methods for Truss Geometry and Topology Design," Struct. Multidiscip. Optim., **7**(3), pp. 141–159.

[11] Bendsøe, M. P., and Sigmund, O., 2004, *Topology Optimization: Theory, Methods, and Applications*, 2nd ed., Springer, Berlin.

[12] Gilbert, M., and Tyas, A., 2003, "Layout Optimization of Large-Scale Pin-Jointed Frames," Eng. Comput., **20**(8), pp. 1044–1064.

[13] Achtziger, W., 2007, "On Simultaneous Optimization of Truss Geometry and Topology," Struct. Multidiscip. Optim., **33**(4–5), pp. 285–304.

[14] Lee, T., Leok, M., and McClamroch, N. H., 2011, "Geometric Numerical Integration for Complex Dynamics of Tethered Spacecraft," American Control Conference, San Francisco, CA, June 29–July 1, pp. 1885–1891.

[15] He, L., and Gilbert, M., 2015, "Rationalization of Trusses Generated Via Layout Optimization," Struct. Multidiscip. Optim., **52**(4), pp. 677–694.

[16] Rozvany, G. I. N., 2009, "A Critical Review of Established Methods of Structural Topology Optimization," Struct. Multidiscip. Optim., **37**(3), pp. 217–237.

[17] Vatanabe, S. L., Lippi, T. N., Lima, C. R. D., Paulino, G. H., and Silva, E. C. N., 2016, "Topology Optimization With Manufacturing Constraints: A Unified Projection-Based Approach," Adv. Eng. Software, **100**, pp. 97–112.

[18] Zhang, W., and Sun, S., 2006, "Scale-Related Topology Optimization of Cellular Materials and Structures," Int. J. Numer. Methods Eng., **68**(9), pp. 993–1011.

[19] Alzahrani, M., Choi, S.-K., and Rosen, D. W., 2015, "Design of Truss-like Cellular Structures Using Relative Density Mapping Method," Mater. Des., **85**, pp. 349–360.

[20] Zhang, P., Toman, J., Yu, Y., Biyikli, E., Kirca, M., Chmielus, M., and To, A. C., 2014, "Efficient Design-Optimization of Variable-Density Hexagonal Cellular Structure by Additive Manufacturing: Theory and Validation," ASME J. Manuf. Sci. Eng., **137**(2), p. 021004.

[21] Degarmo, E., P., Black., J. T., and Kohser, R. A., 2003, *Material and Process in Manufacturing*, 11th ed., John Wiley & Sons, Hoboken, NJ.

[22] Ameta, G., Lipman, R., Moylan, S., and Witherell, P., 2015, "Investigating the Role of Geometric Dimensioning and Tolerancing in Additive Manufacturing," ASME J. Mech. Des., **137**(11), p. 111401.

[23] Gu, D. D., Meiners, W., Wissenbach, K., and Poprawe, R., 2012, "Laser Additive Manufacturing of Metallic Components: Materials, Processes and Mechanisms," Int. Mater. Rev., **57**(3), pp. 133–164.

[24] Diaz, A. R., and Belding, B., 1993, "On Optimum Truss Layout by a Homogenization Method," ASME J. Mech. Des., **115**(3), p. 367

[25] Bendsøe, M. P., 1995, *Optimization of Structural Topology, Shape, and Material*, 1st ed., Springer Verlag, Berlin.

[26] Hajela, P., Lee, E., and Lin, C. Y., 1993, *Genetic algorithms in structural topology optimization* (Topology design of structures, Vol. 227), Springer, Dordrecht, The Netherlands, pp. 117–133.

[27] Wang, M. Y., Wang, X., and Guo, D., 2003, "A Level Set Method for Structural Topology Optimization," Comput. Methods Appl. Mech. Eng., **192**(1–2), pp. 227–246.

[28] Bendsøe, M. P., and Kikuchi, N., 1988, "Generating Optimal Topologies in Structural Design Using a Homogenisation Method," Comput. Methods Appl. Mech. Eng., **71**(2), pp. 197–224.

[29] Sigmund, O., 2001, "A 99 Line Topology Optimization Code Written in Matlab," Struct. Multidiscip. Optim., **21**(2), pp. 120–127.

[30] Sigmund, O., 2009, "Manufacturing Tolerant Topology Optimization," Acta Mech. Sin. Xuebao, **25**(2), pp. 227–239.

[31] Dede, E. M., Joshi, S. N., and Zhou, F., 2015, "Topology Optimization, Additive Layer Manufacturing, and Experimental Testing of an Air-Cooled Heat Sink," ASME J. Mech. Des., **137**(11), p. 111403.

[32] Diaz, A. R., and Kikuchi, N., 1992, "Solutions to Shape and Topology Eigenvalue Optimization Problems Using a Homogenization Method," Int. J. Numer. Methods Eng., **35**(7), pp. 1487–1502.

[33] Sun, C. T., and Vaidya, R. S., 1996, "Prediction of Composite Properties From a Representative Volume Element," Compos. Sci. Technol., **56**(2), pp. 171–179.

[34] Sigmund, O., 1997, "On the Design of Compliant Mechanisms Using Topology Optimization," Mech. Based Des. Struct. Mach., **25**(4), pp. 493–524.

[35] Gaynor, A., Meisel, N. A., Williams, C. B., and Guest, J. K., 2014, "Multiple-Material Topology Optimization of Compliant Mechanisms Created Via PolyJet 3D Printing," ASME J. Manuf. Sci. Eng., **136**(6), pp. 1–10.

[36] Dbouk, T., 2017, "A Review About the Engineering Design of Optimal Heat Transfer Systems Using Topology Optimization," Appl. Therm. Eng., **112**, pp. 841–854.